

Supplementary Notes for Lattice-charge coupling in a trilayer nickelate with intertwined density wave order

Xun Jia,^{1, 2, *} Yao Shen,^{3, †} Harrison LaBollita,^{4, ‡} Xinglong Chen,^{1, §} Junjie Zhang,^{1, ¶} Yu Li,¹ Hengdi Zhao,¹ Mercouri G. Kanatzidis,^{1, 5} Matthew Krogstad,⁶ Hong Zheng,¹ Ayman Said,⁶ Ahmet Alatas,⁶ Stephan Rosenkranz,¹ Daniel Phelan,¹ Mark P. M. Dean,^{3, 7} M. R. Norman,¹ J. F. Mitchell,¹ Antia S. Botana,^{4, **} and Yue Cao^{1, ††}

¹Materials Science Division, Argonne National Laboratory, Lemont, IL 60439, USA

²Multi-disciplinary Research Division, Institute of High Energy Physics, Chinese Academy of Sciences, Beijing 100049, China

³Condensed Matter Physics and Materials Science Department, Brookhaven National Laboratory, Upton, NY 11973, USA

⁴Department of Physics and Astronomy, Arizona State University, Tempe, AZ 85218, USA

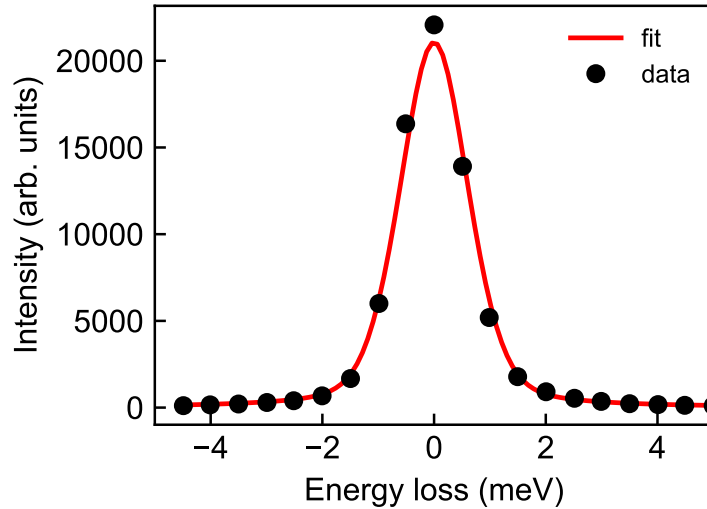
⁵Department of Chemistry, Northwestern University, Evanston, IL 60208, USA

⁶X-ray Science Division, Argonne National Laboratory, Lemont, IL 60439, USA

⁷Department of Physics and Astronomy, The University of Tennessee, Knoxville, Tennessee 37966, USA

1. Energy resolution of the inelastic X-ray scattering measurements

The energy resolution of the inelastic X-ray scattering (IXS) setup was determined by measuring the elastic line using a Kapton tape at 100 K. The IXS spectrum was fitted with a pseudo-Voigt function to determine the energy resolution (Fig. S1).

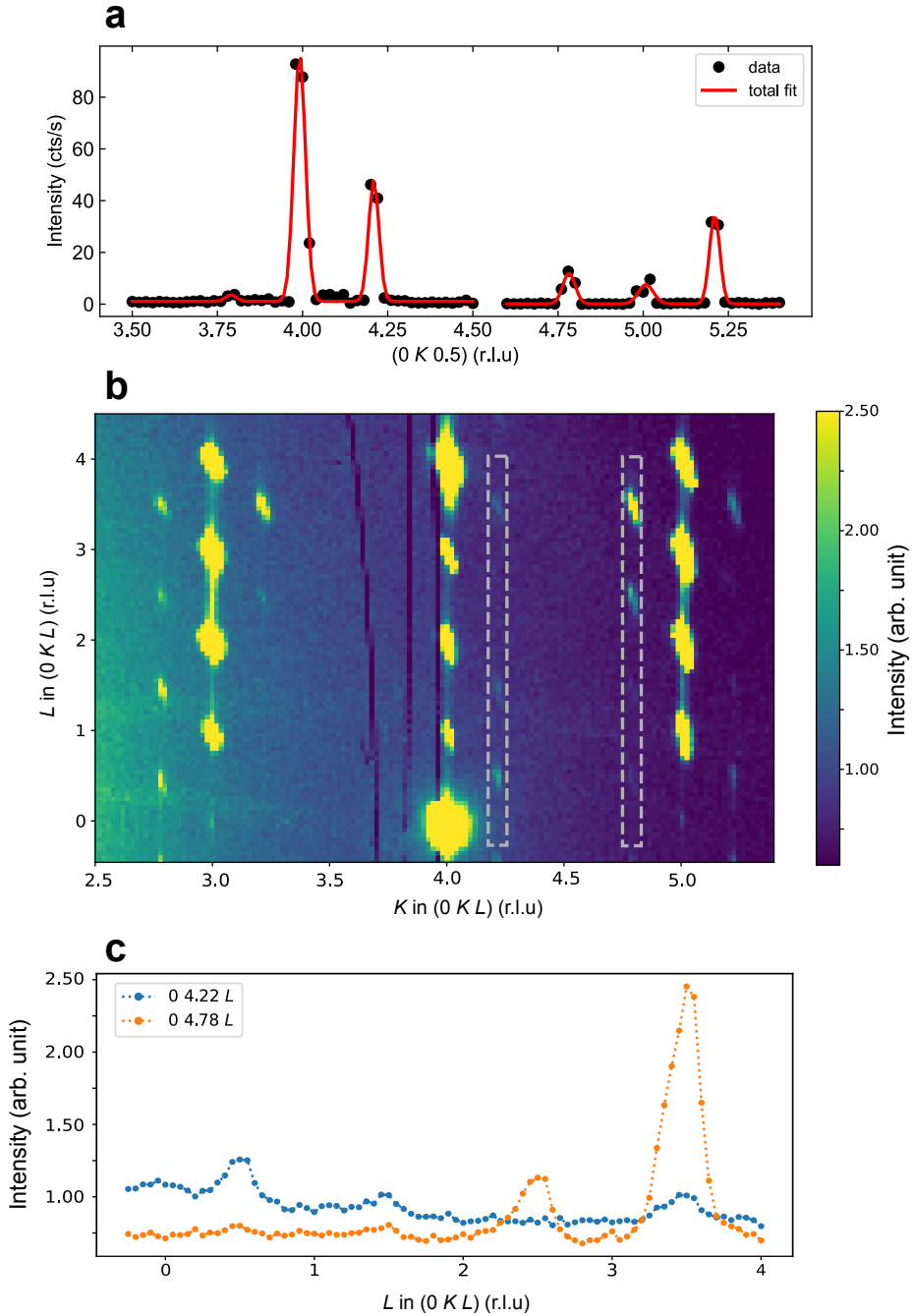


Supplementary Figure 1. The IXS spectrum from a Kapton tape. The black dots and the red solid line correspond to the measured elastic spectrum and the pseudo-Voigt fit, respectively. The energy resolution from the fit is around 1.36 meV.

2. The CDW wavevector for $\text{Pr}_4\text{Ni}_3\text{O}_{10}$

The CDW wavevector was first determined using high-energy X-ray diffraction [1] and then confirmed using IXS with meV energy resolution. Fig. S2(a) shows the elastic scattering intensity from $\text{Pr}_4\text{Ni}_3\text{O}_{10}$ at 100 K along $[0 \ K \ 0.5]_m$ collected during the IXS beamtime. Peaks with non-integer K represent CDW order. Intensities at integer K come from neighboring Bragg peaks with integer L . Fitting confirms that the wavevector of the CDW order has $K=0.79$. The intensity distribution of the CDW order parameter over a larger reciprocal space is displayed in Fig. 2(b) and Fig. 2(c), collected at 100 K at 15-ID-D of the Advanced Photon Source. The CDW peak at $(0 \ 4.22 \ 0.5)_m$ is the

strongest peak in the K range shown in 2(a). The CDW peak at $(0 4.78 3.5)_m$ is stronger, but the structure factor for the dispersive phonon modes away from the elastic line is substantially smaller from the phonony calculation.

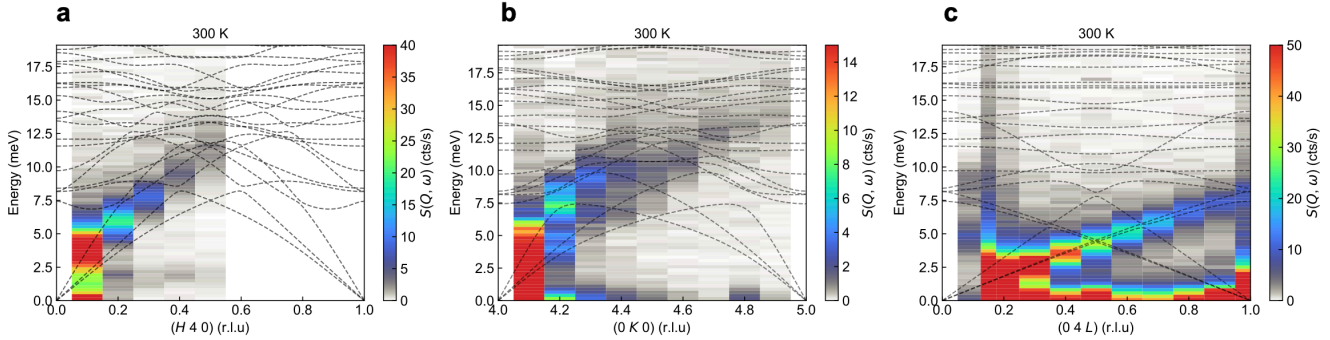


Supplementary Figure 2. Intensity of the CDW peaks in $\text{Pr}_4\text{Ni}_3\text{O}_{10}$ collected (a) using the IXS spectrometer and (b-c) at 30 keV (15-ID-D) with a Pilatus area detector. The cuts in (c) correspond to the long rectangular dashed boxes in (b).

3. Phonon spectra along high symmetry directions for $\text{Pr}_4\text{Ni}_3\text{O}_{10}$

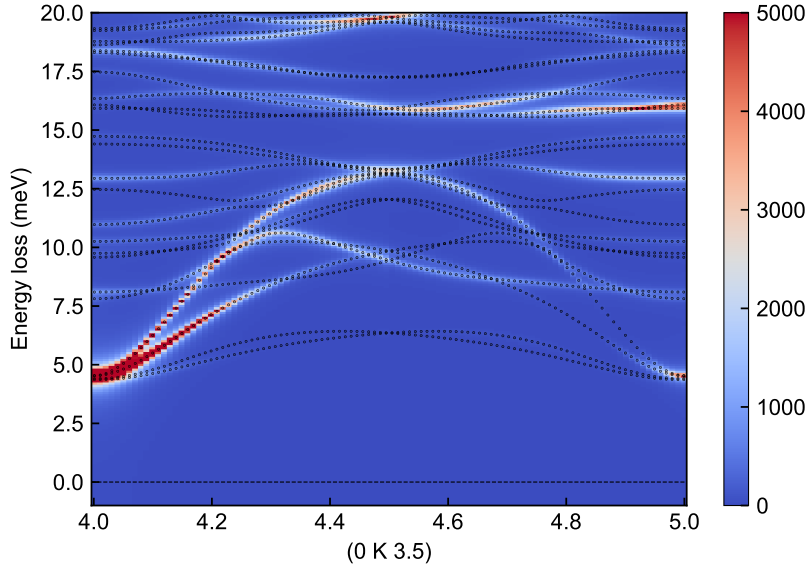
Phonon spectra along H , K , and L under the $P2_1/a$ notation at 300 K are displayed in Fig. S3. The calculated phonon dispersions are represented by dashed black lines, demonstrating a good agreement with the experimental

data.



Supplementary Figure 3. Phonon spectra along (a) $(H, 4, 0)$, (b) $(0, K, 0)$ and (c) $(0, 0, L)$ under the $P2_1/a$ notation measured at 300 K, respectively. The dashed lines are the calculated phonon dispersions.

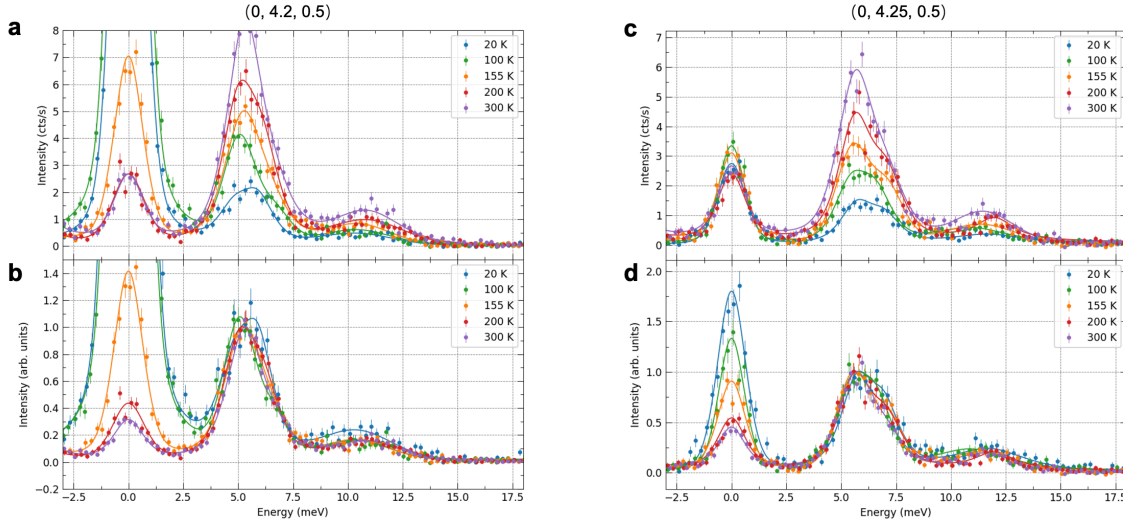
We further calculated the phonon spectra along $(0, K, 3.5)_m$ (Fig. S4). The phonon spectral weight away from the elastic line is small despite the stronger CDW peak at $(0, 4.78, 3.5)_m$. Thus the IXS data at the CDW wavevector was collected near $(0, 4.22, 0.5)_m$ as displayed in the main text.



Supplementary Figure 4. Calculated IXS spectra at $(0, K, 3.5)_m$. Note that the IXS spectral weight at $(0, 4.22, 3.5)_m$ is stronger than that at $(0, 4.78, 3.5)_m$.

4. Temperature dependence of the phonon spectra with and without the Bose factor for $\text{Pr}_4\text{Ni}_3\text{O}_{10}$

The experimentally measured IXS spectrum is proportional to the dynamical structure factor $S(\mathbf{Q}, \omega)$, which has a temperature-dependent Bose prefactor $1/(1 - e^{-\omega/k_B T})$. Fig. S4a and Fig. S4b show the IXS spectra at $(0, 4.2, 0.5)_m$ closest to the \mathbf{Q}_{CDW} before (Fig. S4a) and after (Fig. S4b) removing the Bose factor. The two datasets at $(0, 4.25, 0.5)_m$ are displayed in Fig. S4c and Fig. S4d, respectively. After removing the Bose factor, the IXS spectra show unambiguously that there is no observable phonon softening over the entire temperature range covered in our experiment.



Supplementary Figure 5. (a) and (c) Evolution of the IXS spectra as a function of temperature across the onset of the intertwined order. Panels (b) and (d) display these spectra after the Bose factor correction.

5. Temperature independence of the phonon energies and FWHMs near and away from the CDW wavevector

As outlined in the **Methods** section, we performed a multiple-peak-fitting analysis to obtain the phonon energies and FWHMs as a function of temperature and momentum transfer. Results from the fits are displayed in Fig. S5. These findings, along with the information from Fig. 3 in the main text, indicate that the lack of phonon softening is not limited to the vicinity of Q_{CDW} but extends across a broad momentum range.

6. Phonon spectra near the SDW wavevector for $\text{Pr}_4\text{Ni}_3\text{O}_{10}$

We measured the phonon spectra near one of the SDW wavevectors $\mathbf{Q}_{\text{SDW}}=(2, K, 8.5)_o$ across a wide temperature range from 8 K to 300 K (Fig. S6). A half integer L of 8.5 was selected to capture the SDW peak below ~ 30 K due to magnetic order at the Pr site which also promotes 3D order for the Ni moments [2]. Since the SDW is enhanced with a much longer inter-plane correlation length, $L=8.5$ in principle should shed light on the spin-lattice interactions across the entire temperature range. Despite the many phonon branches, there is no clear indication of phonon softening near \mathbf{Q}_{SDW} .

7. The case of $\text{La}_4\text{Ni}_3\text{O}_{10}$

As mentioned in the main text, we also conducted IXS measurements on a single crystal $\text{La}_4\text{Ni}_3\text{O}_{10}$. The phonon spectra along $(1, K, -0.5)_m$ at 145 K are shown in Fig. S7a, in good agreement with the calculation.

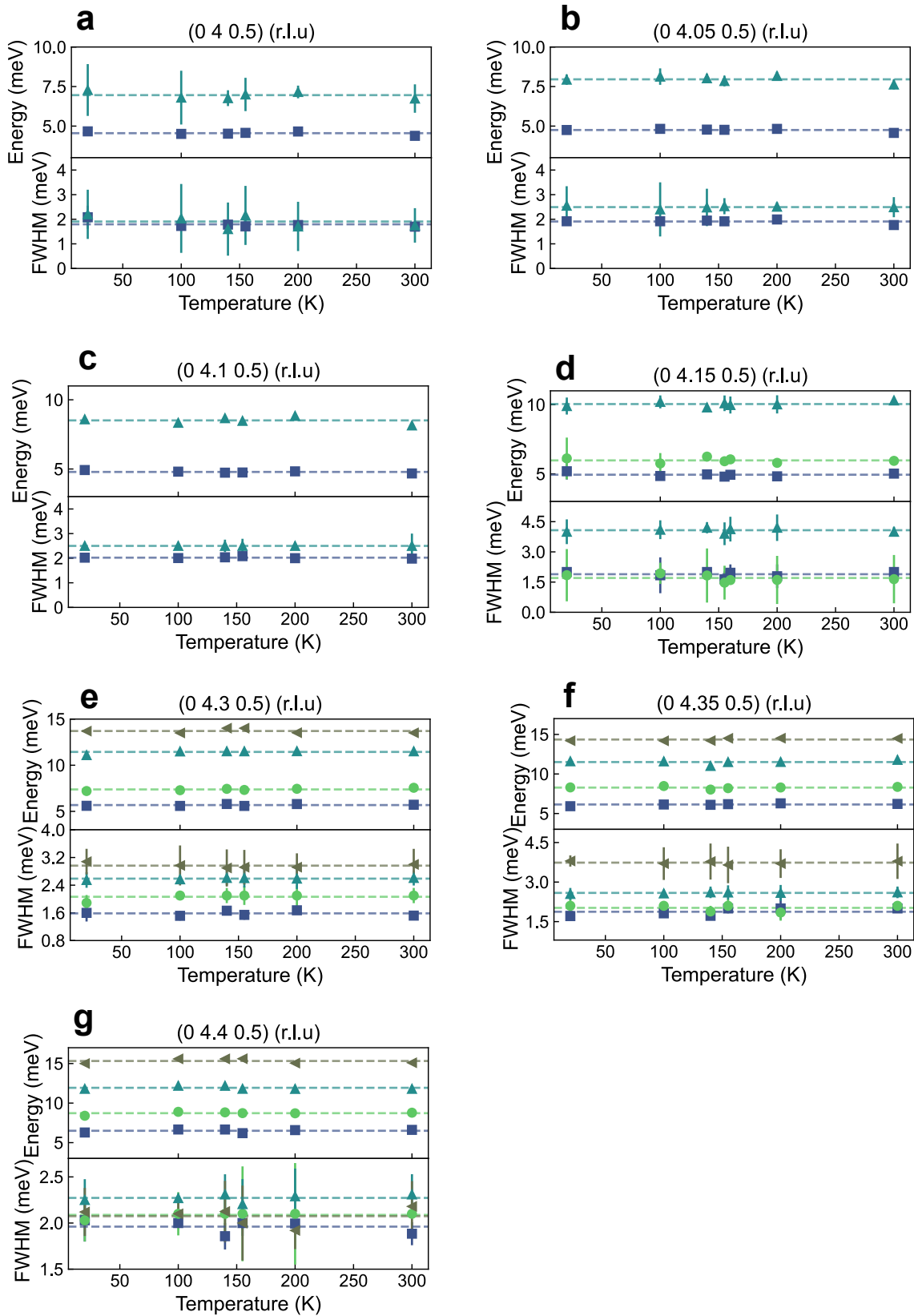
We further collected IXS spectra at $(5, 1.75, -2.5)_m$ across the phase transition (Fig. S7b). Note the CDW wavevector is different for $\text{La}_4\text{Ni}_3\text{O}_{10}$ and $\text{Pr}_4\text{Ni}_3\text{O}_{10}$. The relatively small IXS spectral weight between 5 meV and 10 meV comes from multiple phonon branches. Through detailed fitting, we determined the two higher phonon mode energies to be 14.2 meV and 15.1 meV, respectively. All these phonon modes exhibit no significant temperature dependence, consistent with the observations in $\text{Pr}_4\text{Ni}_3\text{O}_{10}$.

* jiaxun@ihep.ac.cn

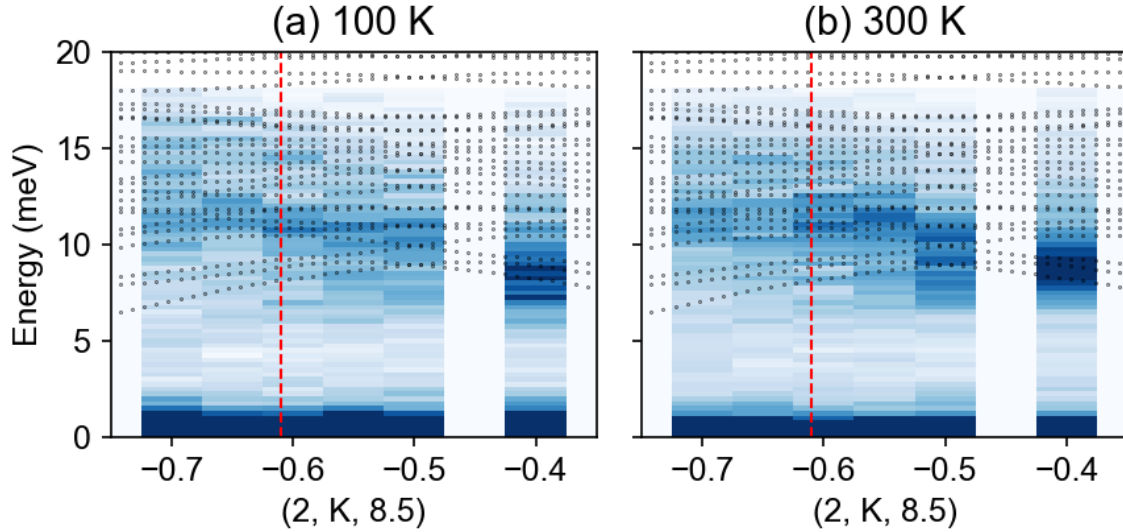
† Present address: Institute of Physics, Chinese Academy of Sciences, Beijing 100190, China

‡ Present address: Center for Computational Quantum Physics, Flatiron Institute, New York, NY 10010, USA

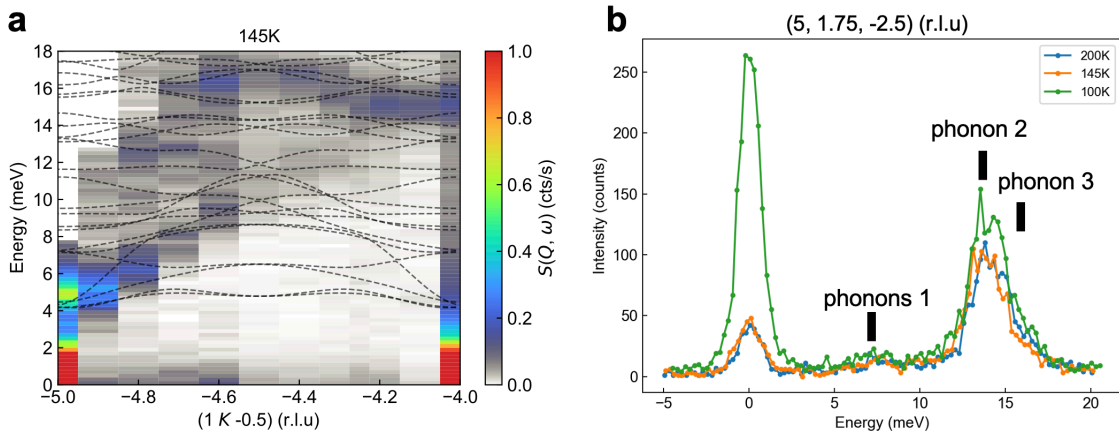
§ Present address: School of Physics, Southeast University, Nanjing, Jiangsu 210096, China



Supplementary Figure 6. Fitted phonon energies and FWHMs along $(0, K, 0.5)_m$ at different temperatures. The error bars are the uncertainties from the fits.



Supplementary Figure 7. Phonon spectra along $(2, K, 8.5)_o$ at (a) 100 K and (b) 300 K. The SDW wavevector is marked using the red vertical dashed line. The calculated phonon dispersions along the same cut are shown using the black solid dots.



Supplementary Figure 8. (a) Phonon spectra along $(1, K, -0.5)_m$ at 145 K. The calculated phonon dispersions along the same cut are shown using the black dashed lines. (b) Temperature dependence of the phonon spectra at $(5, 1.75, -2.5)_m$.

* Institute of Crystal Materials, State Key Laboratory of Crystal Materials, Shandong University, Jinan, Shandong 250100, China

** antia.botana@asu.edu

†† yue.cao@anl.gov

- [1] J. Zhang, D. Phelan, A. Botana, Y.-S. Chen, H. Zheng, M. Krogstad, S. G. Wang, Y. Qiu, J. Rodriguez-Rivera, R. Osborn, *et al.*, Intertwined density waves in a metallic nickelate, *Nat. Commun.* **11**, 6003 (2020).
- [2] A. M. Samarakoon, J. Strempfer, J. Zhang, F. Ye, Y. Qiu, J.-W. Kim, H. Zheng, S. Rosenkranz, M. Norman, J. Mitchell, *et al.*, Bootstrapped dimensional crossover of a spin density wave, *Phys. Rev. X* **13**, 041018 (2023).